JACS
JOURNAL OF THE AMERICAN CHEMICAL SOCIETY
Article
pubs.acs.org/JACS
Terms of Use

Mechanism and Selectivity of Rhodium-Catalyzed 1:2 Coupling of Aldehydes and Allenes

Genping Huang, Marcin Kalek, and Fahmi Himo*

Department of Organic Chemistry, Arrhenius Laboratory, Stockholm University, SE-106 91 Stockholm, Sweden

Supporting Information

ABSTRACT: The rhodium-catalyzed highly regioselective 1:2 coupling of aldehydes and allenes was investigated by means of density functional theory calculations. Full free energy profiles were calculated, and several possible reaction pathways were evaluated. It is shown that the energetically most plausible catalytic cycle is initiated by oxidative coupling of the two allenes, which was found to be the rate-determining step of the overall reaction. Importantly, Rh−allyl complexes that are able to adopt both η^3 and η^1 configurations were identified as key intermediates present throughout the catalytic cycle with profound implications for the selectivity of the reaction. The calculations reproduced and rationalized the experimentally observed selectivities and provided an explanation for the remarkable alteration in the product distribution when the catalyst precursor is changed from $[RhCl(nbd)]_2$ (nbd = norbornadiene) to complexes containing noncoordinating counterions ($[Rh(cod)_2X]$; X = OTf, BF_4, PF_6; cod = 1,5-cyclooctadiene). It turns out that the overall selectivity of the reaction is controlled by a combination of the inherent selectivities of several of the elementary steps and that both the mechanism and the nature of the selectivity-determining steps change when the catalyst is changed.

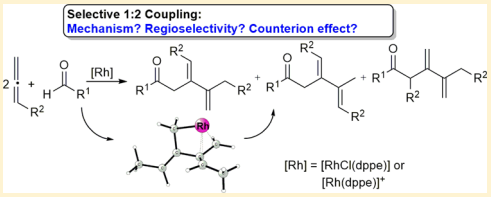

1. INTRODUCTION

Rhodium(I) complexes are well-established catalysts for three-component cycloadditions of unsaturated compounds, yielding carbocycles with various ring sizes (e.g., six-membered; Scheme 1a).[1] Rhodium(I) also catalyzes hydroacylation reactions in which an acyl unit and the hydrogen atom of an aldehyde are added across a C−C multiple bond (Scheme 1b).[2] A reductive version of the latter process, furnishing the corresponding alcohols, has also been developed (Scheme 1c).[3] In 2006, Krische and co-workers reported a novel reaction that can be considered as a crossover between those presented in Scheme 1a and Scheme 1c. In its course, two molecules of acetylene are coupled with one molecule of aldehyde under a hydrogen atmosphere to form a linear allylic alcohol product (Scheme 2a).[4,5] Very recently, a combination of the in principle more fundamental couplings from Scheme 1a,b has also been successfully accomplished.[6,7] In particular, a significant example comes from the laboratory of Murakami and consists of a 1:2 coupling of aldehydes and allenes (Scheme 2b).[6]

Scheme 1

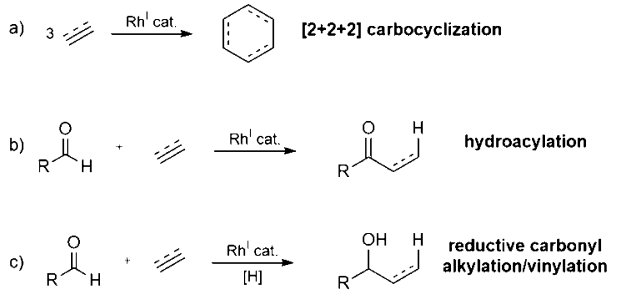

The reaction in Scheme 2b indeed constitutes a state-of-the-art method in synthetic organic chemistry. It is inherently atom-economical and leads to a large increase in molecular complexity in a single step. A particularly appealing feature of this process is its selectivity, which is a much more complex issue than in the reaction involving acetylene (Scheme 2a). Considering only the couplings of two monosubstituted allene moieties of type **2** with one molecule of aldehyde **1**, 36 different isomers of the product are possible, with various connectivities and *Z*/*E* arrangements of the double bonds.[8] Experimentally, when $[RhCl(nbd)]_2$ (nbd = norbornadiene) was used as the rhodium source and 1,2-bis(diphenylphosphino)ethane (dppe) as the ligand, product **3** was obtained with 91% selectivity, accompanied by two minor isomers, **4** (6%) and **5** (3%).[6] Very interestingly, when the chloride was replaced by a non-coordinating counterion such as TfO^-, BF_4^-, or PF_6^-, the selectivity of the reaction was switched, and compound **5** became the dominant product (87−95%).[6] The common features of the products obtained under the two sets of reaction conditions are that the two allene moieties are coupled through their central atoms (C2−C2 linkage) and the aldehyde is attached to one of the terminal carbons (C1 or C3) of one of the allenes.

The reaction mechanism of the related three-component reductive coupling shown in Scheme 2a has been investigated by a combination of experimental and computational

Received: February 7, 2013
Published: April 25, 2013

   dx.doi.org/10.1021/ja4014166 | J. Am. Chem. Soc. 2013, 135, 7647−7659

Scheme 2

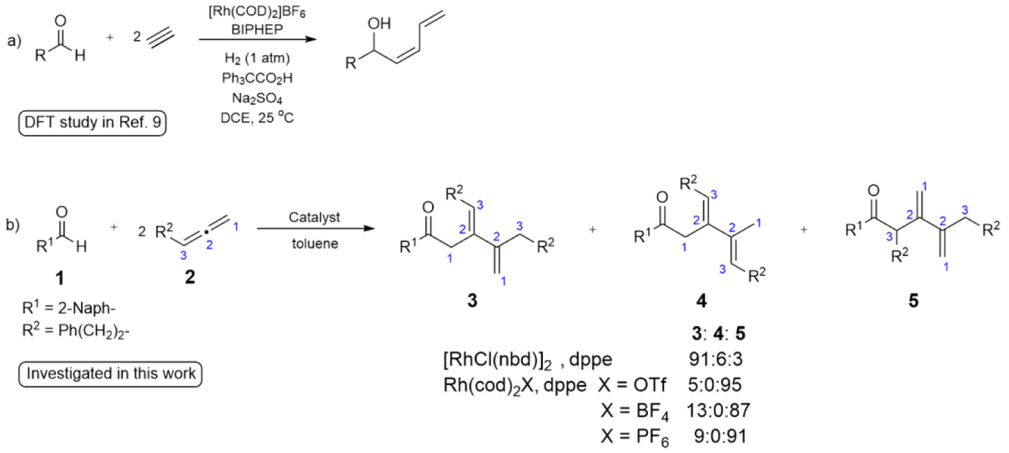

Scheme 3. Possible General Mechanistic Pathways for the Reaction in Scheme 2b, As Suggested by Experimental Findings or Proposed in the Literature[a]

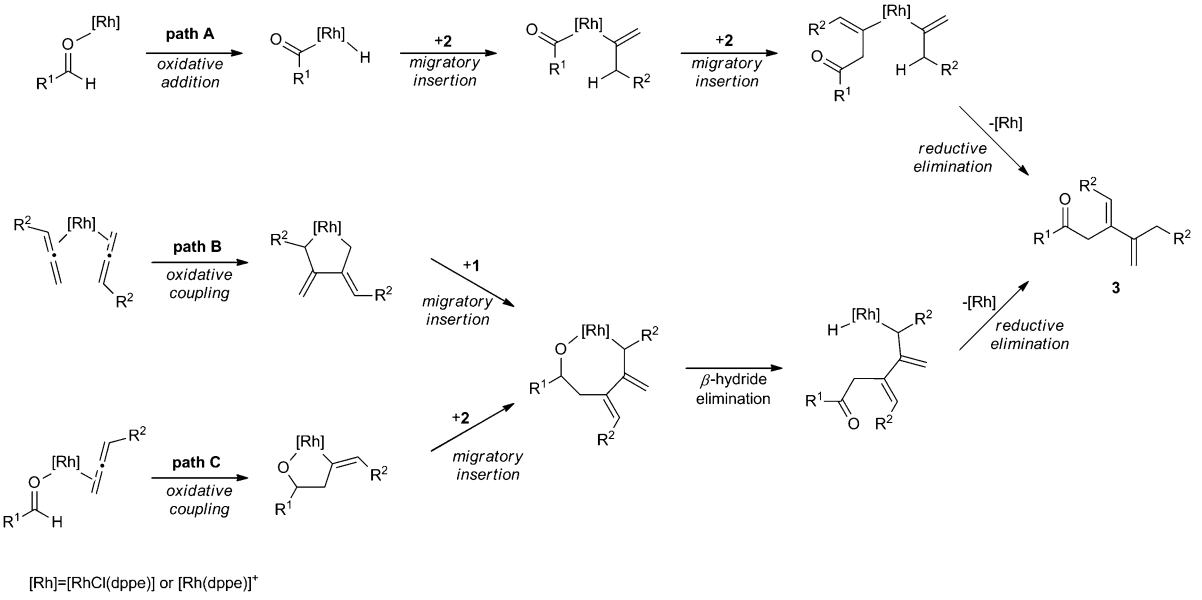

[a]Each of the three pathways can yield all of the possible products. Here, only the routes leading to product **3** are shown.

approaches.[9] It was established the reaction takes place via an initial oxidative coupling of two acetylene molecules followed by migratory insertion of the aldehyde molecule, hydrogenolysis, and reductive elimination.[9] Hence, except for the extra hydrogenolysis step, this mechanism is similar to the well-established catalytic cycle of the trimerization process depicted in Scheme 1a.[1d]

In the case of the 2:1 coupling of allenes and aldehydes (Scheme 2b), it is not evident that an analogous mechanistic pathway is followed. It has been shown experimentally that allenes of type **2** indeed undergo an initial oxidative coupling in the presence of a Rh(I) catalyst, but instead of the subsequent migratory insertion that would eventually result in the regular [2 + 2 + 2] cycloaddition (Scheme 1a), a β-hydride elimination/reductive elimination sequence occurs, leading overall to a linear dimer.[10,11] Additionally, it is known that the hydroacylation reactions (Scheme 1b) are initiated by oxidative addition of aldehydes to Rh(I) complexes,[2a] so this process may also be involved in the mechanism of the combined reaction shown in Scheme 2b. Finally, there is also an additional possibility of an initial oxidative coupling between the aldehyde and the allene moieties that has been shown to take place in some catalytic cycles.[12] A mechanism starting with the oxidative coupling of aldehyde and allene was actually suggested by Murakami and co-workers in their report.[6]

These possible mechanisms for the reaction, suggested by the experimental findings or proposed in the literature, are summarized in Scheme 3. They differ in regard to the initial step, which is either C−H oxidative addition, allene−allene oxidative coupling, or aldehyde−allene oxidative coupling. In addition to the general mechanism, there is the issue of the reaction selectivity and its sources. Each of the pathways shown in Scheme 3 may yield each of the 36 possible product isomers, including the experimentally observed **3**, **4**, and **5**, by simply altering the positions at which the new bonds are formed. Moreover, all three pathways are consistent with the results of deuterium labeling studies carried out experimentally.[6] In addition, for almost all of the intermediates in Scheme 3 one

dx.doi.org/10.1021/ja4014166 | J. Am. Chem. Soc. 2013, 135, 7647−7659

can envision alternative reactions that they may undergo (not shown in the scheme) leading to side products with entirely different structures (e.g., **1**−**2** or **2**−**2** dimers, etc.), which adds to the complexity of the system.

Considering the significance of the coupling reaction depicted in Scheme 2b and the current poor understanding of its mechanism, in particular the origins of the observed selectivity, we decided to investigate it computationally by means of density functional theory (DFT). The calculations showed that the reaction indeed initially follows the pathway starting with oxidative coupling of two allene molecules (Scheme 3, path B). However, we found that a not previously suggested allylation of the aldehyde takes place subsequently with important selectivity implications. It is shown that a key role in the reaction mechanism is played by rhodium complexes containing allyl ligands that can adopt either η^3 or η^1 coordination, which display intrinsically distinct reactivities. Moreover, it is demonstrated that the reaction catalyzed by rhodium complexes with noncoordinating counterions follows a partially different mechanistic route involving an alkoxide oxidation step. The calculations provide an explanation for the observed selectivity switch when the counterion in the Rh catalyst is altered.

2. COMPUTATIONAL DETAILS

All of the calculations were performed using the Gaussian 03 package[13] and the B3LYP functional.[14] Geometry optimizations were done with a combined basis set in which the LANL2DZ basis set with pseudopotential[15] was used for Rh and the 6-31G(d,p) basis set was used for all other atoms. Frequencies were computed analytically at the same level of theory to confirm whether the structures were minima (no imaginary frequencies) or transition states (only one imaginary frequency). Selected transition-state structures were confirmed to connect the correct reactants and products by intrinsic reaction coordinate (IRC) calculations. To obtain better accuracy of the final energy values, the energies of the optimized geometries were recalculated using single-point calculations with a larger basis set, namely, LANL2DZ for Rh and 6-311+G(2d,2p) for the other atoms. The effect of solvation was evaluated by performing single-point self-consistent reaction field calculations with the conductor-like polarizable continuum model (C-PCM)[16] as implemented in Gaussian 03. The parameters for toluene (ε = 2.379), corresponding to the experimental conditions, and the united atom (UA0) radii were used in these calculations.

The final Gibbs energies reported in the article (ΔG_{Tol}) are the large-basis-set single-point energies with Gibbs energy corrections (at 298.15 K), solvation corrections, and corrections for dispersion effects using the method of Grimme.[17] Inclusion of the dispersion effects has recently been shown to improve the performance of the B3LYP method significantly.[18]

The calculations were carried out using the full structure of the dppe ligand, while the aldehyde and allene reactants were represented with smaller model structures, namely, benzaldehyde (**1**, R^1 = Ph in Scheme 2b) and buta-1,2-diene (**2**, R^2 = Me), respectively.

3. RESULTS AND DISCUSSION

Because of the number of possible mechanistic pathways (Scheme 3), the reaction poses a considerable challenge from a computational point of view. In this section, we first focus on the [RhCl(dppe)]-catalyzed reaction, assuming that chloride is coordinated to the metal center. The mechanism of the reaction is systematically examined step by step by evaluating all of the possible pathways, including potential side reactions. After the overall mechanism is established, the full catalytic cycle and the energy profile are summarized and the origins of the regioselectivity are discussed. In the final part, we present the results of the calculations on the reaction catalyzed by the cationic $[Rh(dppe)]^+$ complex, which is the putative active species in the reactions using catalyst precursors containing noncoordinating counterions. The obtained free energy profile is then analyzed, and the origins of the observed alteration of the selectivity when the catalyst is changed are explained.

All of the free energies are reported relative to the sum of the free energies of the free reactants and catalyst (i.e., **1** + 2 × **2** + [Rh], where [Rh] = [RhCl(dppe)] or $[Rh(dppe)]^+$), which we have chosen to set equal to zero.

3.1. Initial Step of the Catalytic Cycle: Oxidative Coupling versus Oxidative Addition. Before considering the various reaction pathways, we evaluated the different modes of binding between the catalyst and the reactants. The calculations showed that coordination of allene **2** to the Rh catalyst to give **INT1** is exergonic by 8.9 kcal/mol, whereas binding of aldehyde **1** to form **INT1a** is exergonic by 1.6 kcal/mol (Figure 1). The introduction of any additional ligands

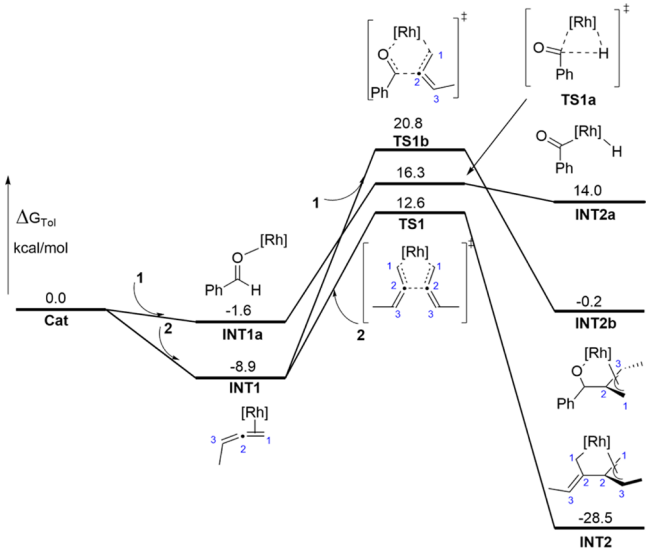

Figure 1. Free energy profiles for the possible initial steps of the reaction. The intermediates connecting **INT1** with **TS1** and **TS1b** were found to be higher in free energy than **INT1**, so they are not shown in the diagram (see the Supporting Information for details).

always resulted in an increase in the free energy, which is in agreement with the known preference of d^8 metal complexes to adopt a four-coordinate square-planar geometry (see the Supporting Information). Hence, **INT1** containing a single allene molecule, dppe, and chloride as ligands (see Figure 2 for the structure) is the lowest-energy Rh(I) species, to which the barriers for the initial step should be related.

As shown in Scheme 3, three general mechanistic pathways for the investigated reaction are possible, each of which begins with a different step, namely, C−H oxidative addition (path A), allene−allene oxidative coupling (path B), or aldehyde−allene oxidative coupling (path C). We optimized the transition states (TSs) corresponding to these steps and compared them in terms of their relative free energies, taking into account all of the possible coupling patterns of the reactants where applicable.

The C−H oxidative addition of aldehyde (path A in Scheme 3) was found to take place via transition state **TS1a** (Figure 2). It requires overcoming an overall barrier of 25.2 kcal/mol relative to **INT1** and involves an initial interconversion into the

dx.doi.org/10.1021/ja4014166 | J. Am. Chem. Soc. 2013, 135, 7647−7659

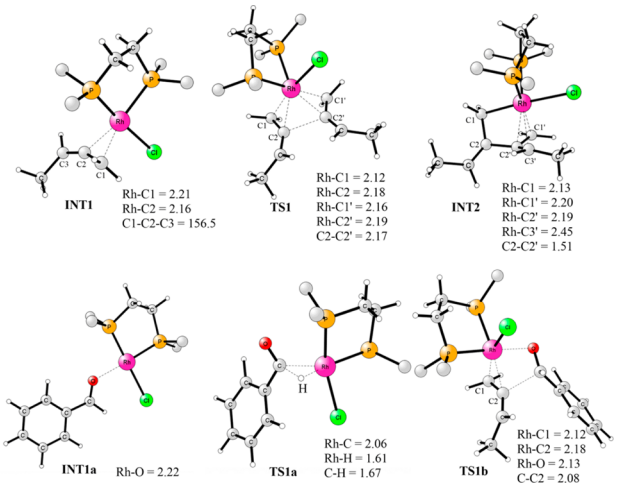

Figure 2. Optimized structures of selected intermediates and transition states for the initial step (distances in Å and angles in deg). For clarity, the phenyl substituents on the phosphorus centers have been omitted in the figure.

aldehyde-containing complex **INT1a** (Figure 1). The oxidative addition results in the formation of the Rh(III) hydride **INT2a**, and the process is endergonic by as much as 22.9 kcal/mol.

The oxidative coupling of two allene moieties (path B in Scheme 3) was much more complicated to investigate than the oxidative addition. In the course of this step, the C−C bond formation may occur between any of the three carbon atoms of each of the coupling partners (C1−C1, C1−C2, C1−C3, C2−C1, etc.). Additionally, when the central atom of the allene (C2) is engaged in the C−C bond formation, extra combinations arise from the fact that either of the terminal carbons (C1 or C3) may bind to the rhodium center. When the *Z*/*E* arrangements of the double bonds and, in three cases, the cis/trans isomers are also taken into account, there are in total 24 distinct TSs that must be considered (Scheme 4). The free energies for all of these were calculated, and the one with the lowest free energy was found to be **TS1**, whose structure is shown in Figure 2 (structures and energies of all of the TSs are given in Supporting Information). In this TS, the rhodium center, which constitutes the largest steric bulk in the system because of the proximity of the phenyl-substituted phosphine ligand, is coordinated to the least-substituted carbons (C1) of the allenes. Additionally, the *Z*,*Z* arrangement of the double bonds minimizes the repulsion in the other part of the structure. The free energy of **TS1** was calculated to be 21.5 kcal/mol higher than that of **INT1** (Figure 1). The free energies of the other TSs shown in Scheme 4 were calculated to be higher than that of **TS1** by at least 2.2 kcal/mol (see the Supporting Information).

Scheme 4. Possible Transition States for Oxidative Coupling of the Two Allene Moieties[a]

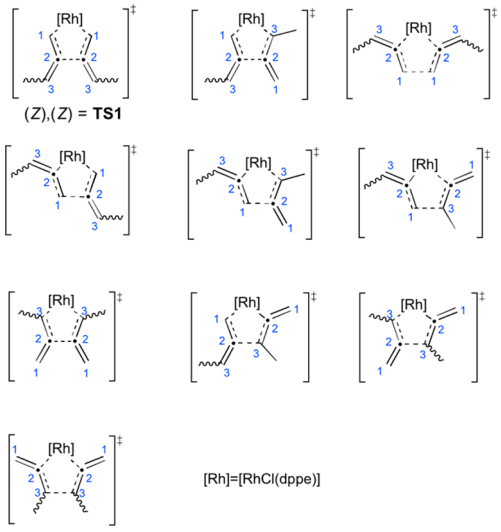

[a]It should be noted that for each of the TS structures there are varying numbers of *Z*/*E* or cis/trans isomers, resulting in an overall total of 24 possible TSs.

Interestingly, **TS1** does not lead to the expected five-membered metallacycle but instead yields an octahedral Rh(III) complex **INT2**, containing an η^3-allyl-η^1-allyl ligand (see Figure 2 for the structure).[19] In what follows, we will refer to this kind of intermediate as η^3,η^1-bis(allylic), in accordance with the literature.[20] The formation of **INT2** is exergonic by 19.6 kcal/mol relative to **INT1**. This kind of η^3,η^1-bis(allylic) ligand could be expected to undergo syn/anti isomerization of the methyl substituents. However, intermediate **INT2** possesses some unique features that result in the preservation of its stereochemical configuration as formed in the course of the reaction from **TS1** (i.e., *Z* double-bond geometry and anti CH_3 group in the η^3-allyl system). First, the methyl substituent in the η^3-allyl of **INT2** cannot move from the anti position to the syn position via an $\eta^3-\eta^1-\eta^3$ isomerization mechanism, as the required rotation in the transient η^1 complex is impossible because the allylic system is a part of metallacycle. Second, it is possible for the η^3 and η^1 allyl groups in **INT2** to exchange places, but this also maintains the overall configuration. During such a process, the anti CH_3 group becomes a substituent of the *Z*-configured double bond and vice versa. Finally, **INT2** may transiently be transformed into an isomeric η^3,η^1-bis(allylic) complex, **INT2′**, that is calculated to be 8.5 kcal/mol higher in free energy than **INT2** (Scheme 5). However, such an interconversion also leaves the stereochemical arrangement of the allene dimer moiety intact. These properties are of importance for the overall selectivity of the reaction, as will be discussed below.

As a final option for the initial step, oxidative coupling between the aldehyde and allene molecules was also examined (path C in Scheme 3). Similar to the case of allene−allene oxidative coupling, the C−C bond may be formed between the carbonyl carbon and positions C1, C2, or C3 of the allene. When the Rh coordination as well as the *Z*/*E* and cis/trans isomers are also considered, there are seven possible transition states (see the Supporting Information). The one with the lowest free energy among them is **TS1b** (Figure 2). The corresponding free energy barrier is 29.7 kcal/mol from **INT1**, and the formation of the resulting Rh(III) complex **INT2b** is endergonic by 8.7 kcal/mol relative to **INT1** (Figure 1).

These results clearly point to oxidative coupling of the two allenes leading to intermediate **INT2** as the favored initial step of the mechanism. The transition state for the C−H oxidative addition (**TS1a**) is 3.7 kcal/mol higher than **TS1** (but lower than many of the transition states depicted in Scheme 4). On the other hand, the oxidative coupling between the aldehyde and allene was found to occur via high-energy transition states, the lowest of which (**TS1b**) is 8.2 kcal/mol higher than **TS1**. Importantly, the formation of **INT2** is irreversible, and therefore, already at this point it is possible to dismiss paths

dx.doi.org/10.1021/ja4014166 | J. Am. Chem. Soc. 2013, 135, 7647−7659

Scheme 5. Possible η^3–η^1–η^3 Isomerization of INT2[a]

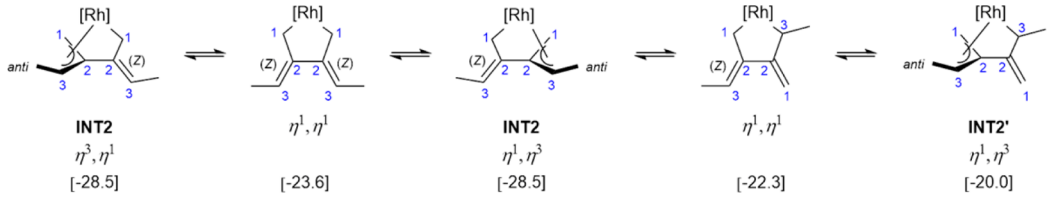

[a]Free energies relative to the global zero are indicated in kcal/mol.

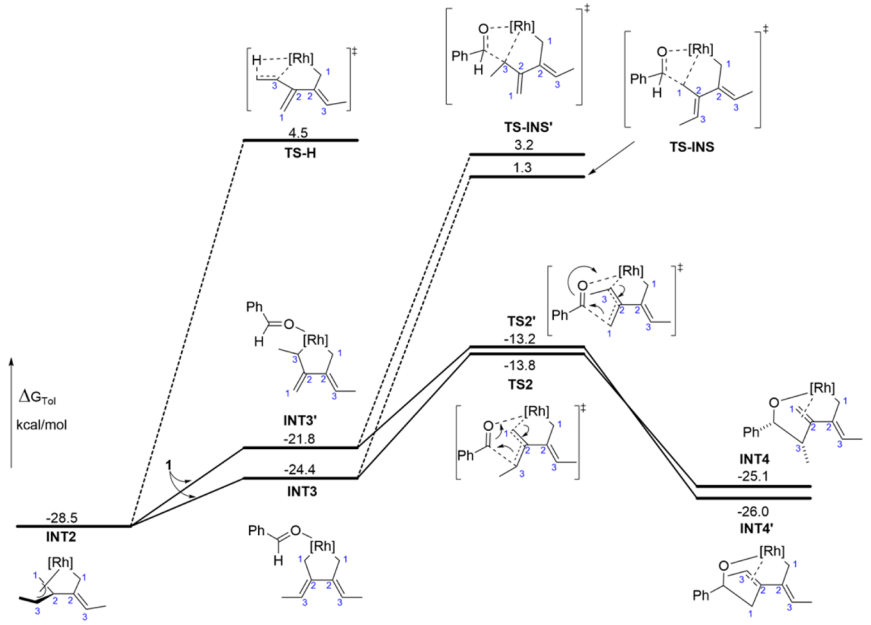

Figure 3. Free energy profile for the formation of the second C–C bond.

A and C of Scheme 3 as plausible reaction mechanisms. Using the same argument, one can also discard all of the pathways starting with oxidative coupling of the two allenes in arrangements other than in **TS1** (Scheme 4). Hence, from the reaction mixture containing the Rh(I) catalyst (**cat**), aldehyde **1**, and allene **2**, intermediate **INT2** should be formed practically exclusively. As explained above, this intermediate has a defined stereochemical configuration that strongly narrows the number of possible final products of the reaction. In the following sections, we will show that the experimentally observed product **3**, as well as the minor side products **4** and **5**, can all be derived from **INT2** as a common precursor.

3.2. Formation of the Second C–C Bond. Once the two allene molecules are coupled in the first step of the mechanism to form **INT2**, the second C–C bond formation must take place, incorporating the aldehyde moiety into the structure and thus assembling the complete backbone of the product. It has been suggested that the second C–C bond formation should occur via migratory insertion of the aldehyde into the Rh–C bond.[6] Such a course of the reaction was also established in mechanistic studies on the above-mentioned related reductive 2:1 coupling of acetylenes with aldehydes (Scheme 2a).[9] In addition to insertion of the aldehyde, **INT2** may potentially undergo a competing process, namely, a β-hydride elimination that would eventually lead to the formation of the dimer of allene **2**. There is experimental evidence that the latter pathway is followed in the absence of aldehyde **1** in the reaction mixture.[10] In the present study, we discovered an additional alternative for the C–C bond formation that has not been proposed previously and that turns out to have a much lower barrier than the two other processes. This alternative pathway involves direct allylrhodium addition to the aldehyde. In this section, these mechanistic possibilities are investigated and compared.[21]

Irrespective of the specific way the new C–C bond is formed, the reaction begins with the coordination of aldehyde **1** to the rhodium center. To create the necessary coordination site for the aldehyde, the allyl ligand must change its binding mode from η^3 to η^1. This may occur in two distinct ways, with either C1 or C3 ligating the metal center in the resulting complex (**INT3** or **INT3′**, respectively; Figure 3). This transformation was calculated to be endergonic by 4.1 and 6.7 kcal/mol, respectively.

From **INT3**, the migratory insertion may occur only at the C1 position because of the symmetric structure of this intermediate, while on the other hand, insertion in **INT3′** can take place at either C1 or C3. The calculations showed that the lowest-energy transition state leads to the insertion at C1 (**TS-INS**) and arises from **INT3**. The second-lowest transition state found was **TS-INS′**, which involves the insertion at C3 from **INT3′**. The corresponding barriers for **TS-INS** and **TS-INS′** relative to **INT2** are 29.8 and 31.7 kcal/mol, respectively (Figure 3). The free energy difference between them can be explained by the steric repulsion between the proximal methyl group and the aldehyde in the latter transition state.

dx.doi.org/10.1021/ja4014166 | J. Am. Chem. Soc. 2013, 135, 7647–7659

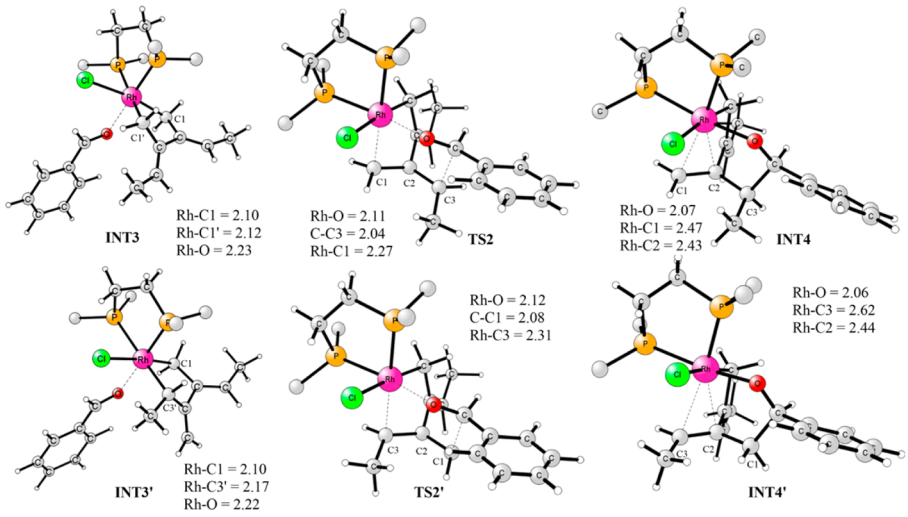

Figure 4. Optimized structures of the allylation reactants, transition states, and resulting complexes.

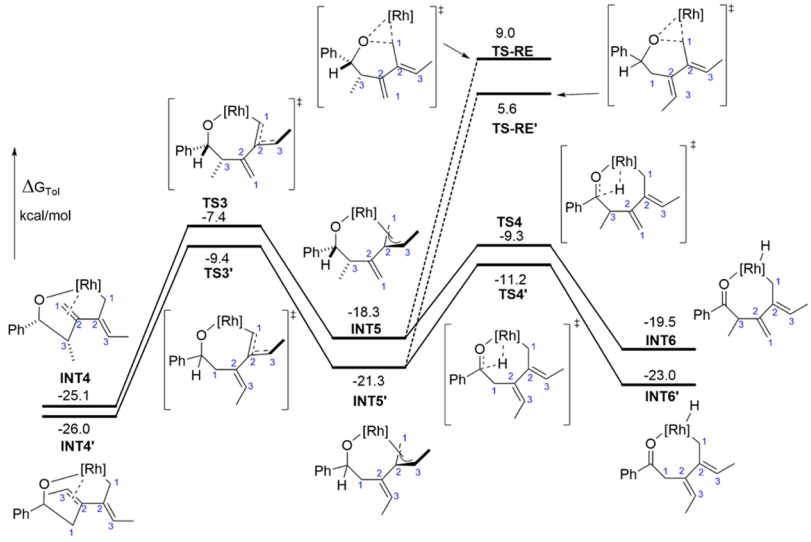

Figure 5. Free energy profile for the β-hydride elimination step.

The alternative C−C bond formation pathway that we discovered to be possible starting from **INT3** or **INT3′** is a direct attack of the σ-allyl ligand on the aldehyde coordinated to the rhodium center.[22] Such a reaction, which occurs via a six-membered cyclic transition state (**TS2** or **TS2′**, respectively; see Figure 3 for schematic illustrations and Figure 4 for optimized structures), was found to be energetically more favorable than the migratory insertion by as much as 15 kcal/mol.

In this case, the C−C bond formation from **INT3** can occur only at the C3 position (**TS2**). The corresponding barrier was calculated to be 14.7 kcal/mol relative to **INT2**. However, allylation from **INT3′** may take place at either C1 or C3, but the former scenario is lower in free energy (**TS2′** in Figure 3) and requires overcoming an overall barrier of 15.3 kcal/mol relative to **INT2**. In both **TS2** and **TS2′**, the six-membered ring adopts the chairlike geometry (Figure 4) with the methyl and phenyl groups occupying the axial and equatorial positions, respectively. The small free energy difference between them might be explained by a steric repulsion between the methyl group and the Rh center in **TS2′**, which is not present in **TS2**. Transition states **TS2** and **TS2′** constitute the divergence point from which the reaction proceeds along two separate parallel pathways.

The allylations occurring via **TS2** and **TS2′** yield octahedral complexes **INT4** and **INT4′**, respectively, containing η^2-alkene and alkoxide ligands coordinated to Rh(III) (see Figure 4 for optimized structures). Interestingly, **INT4** was found to be 0.9 kcal/mol less stable than **INT4′**.

Finally, the β-hydride elimination from **INT2**, the possible side reaction at this stage of the mechanism, was found to have a barrier of 33.0 kcal/mol relative to **INT2** (via **TS-H**, whose optimized structure is given in the Supporting Information), which is 18.3 kcal/mol higher than that found for **TS2** (Figure 3). Therefore, in the presence of aldehyde **1** in the reaction mixture, the allylation is expected to occur much more favorably, in agreement with the experimental results.

3.3. β-Hydride Elimination. The next step in the reaction pathway is the β-hydride elimination, which restores the carbonyl group (Scheme 3, path B). In both **INT4** and **INT4′**, the only β-hydrogen available is the one originating from the aldehyde group, and hence, it will be exclusively transferred to the metal center. However, for the β-hydride elimination to take place, a vacant coordination site must be created to

dx.doi.org/10.1021/ja4014166 | J. Am. Chem. Soc. 2013, 135, 7647−7659

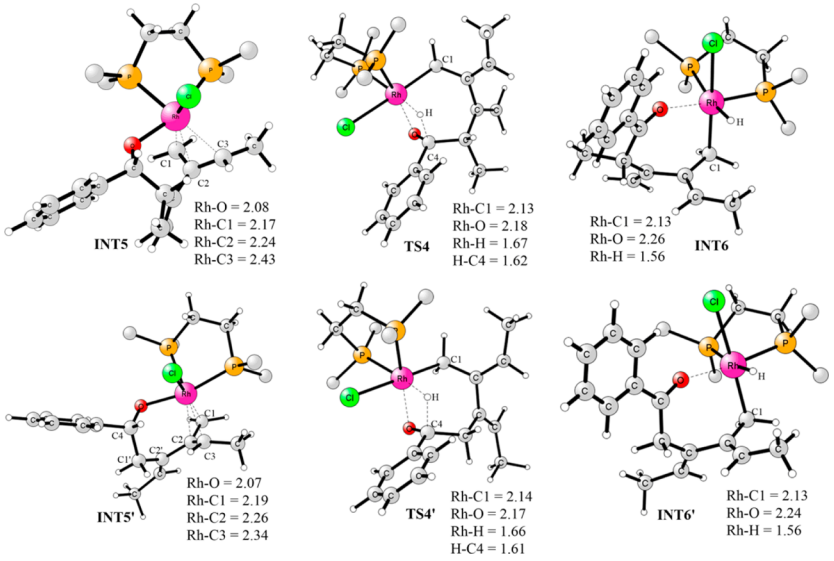

Figure 6. Optimized structures of the β-hydride elimination transition states and the resulting η^1-allyl complexes.

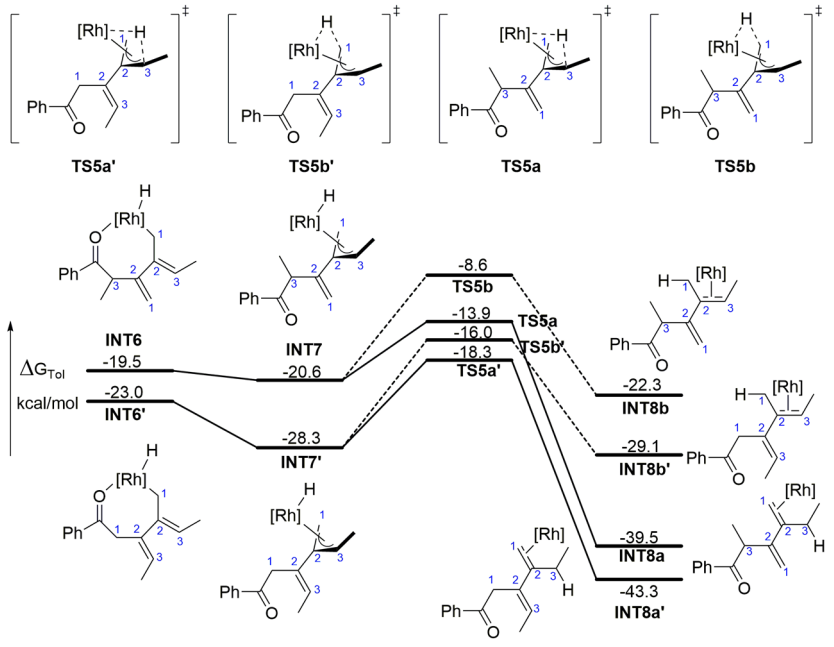

Figure 7. Free energy profile for the reductive elimination step.

accommodate the hydride. This can be generated by dissociation of the η^2-alkene from the metal center in **INT4** and **INT4′** followed by rotation of the alkoxide ligand. The calculations showed that this isomerization takes place through a series of steps, among which the highest-energy transition states are **TS3** and **TS3′** with barriers of 17.7 and 16.6 kcal/mol relative to **INT4** and **INT4′**, respectively (Figure 5). A detailed description of the isomerization process, together with calculated free energy profiles and optimized structures, can be found in the Supporting Information.

The isomerization results in intermediates **INT5** and **INT5′** containing an η^3-allyl ligand, which were calculated to be higher in free energy by 6.8 and 4.7 kcal/mol relative to **INT4** and **INT4′**, respectively. From **INT5** and **INT5′**, the β-hydride elimination takes place with a simultaneous change in the coordination mode of the allyl group from η^3 to η^1 in order to create a vacant site for the hydride at the metal center (**TS4** and **TS4′**; see Figure 6 for optimized structures). The calculated free energies of **TS4** and **TS4′** relative to the respective intermediates **INT5** and **INT5′** are 9.0 and 10.1 kcal/mol (Figure 5), respectively. It should be noted that transitions states **TS4** and **TS4′** are lower in free energy than the preceding **TS3** and **TS3′**, which is of importance for the analysis of the selectivity (see below). The rhodium hydride complexes resulting from the β-elimination (**INT6** and **INT6′**) are octahedral and contain an η^1-allyl and a carbonyl oxygen coordinated to the metal.

We also considered an alternative process that theoretically may interfere with the β-hydride elimination from **INT5** or **INT5′**, namely, a C−O bond-forming reductive elimination. With such a course, the reaction would yield pyrane derivatives as products and thus would constitute a heteroatom analogue of the [2 + 2 + 2] carbocyclization shown in Scheme 1a.[23] However, the calculated barrier for this process (from **INT5′** to

dx.doi.org/10.1021/ja4014166 | J. Am. Chem. Soc. 2013, 135, 7647−7659

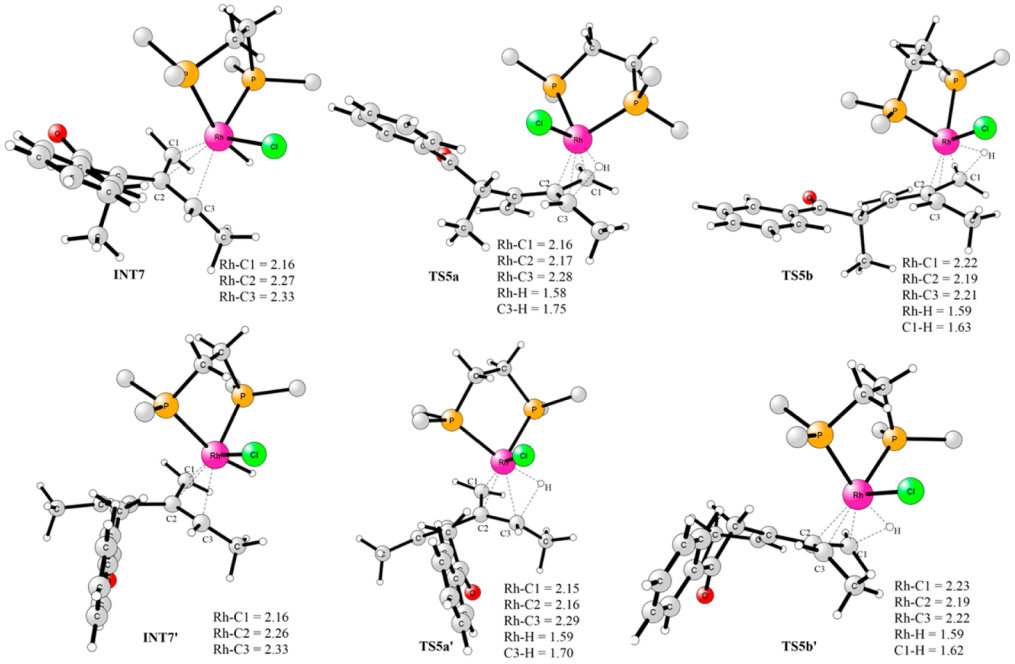

Figure 8. Optimized structures of the reductive elimination reactants and transition states.

Scheme 6. Summary of the Mechanism of the [RhCl(dppe)]-Catalyzed 1:2 Coupling of Aldehydes and Allenes

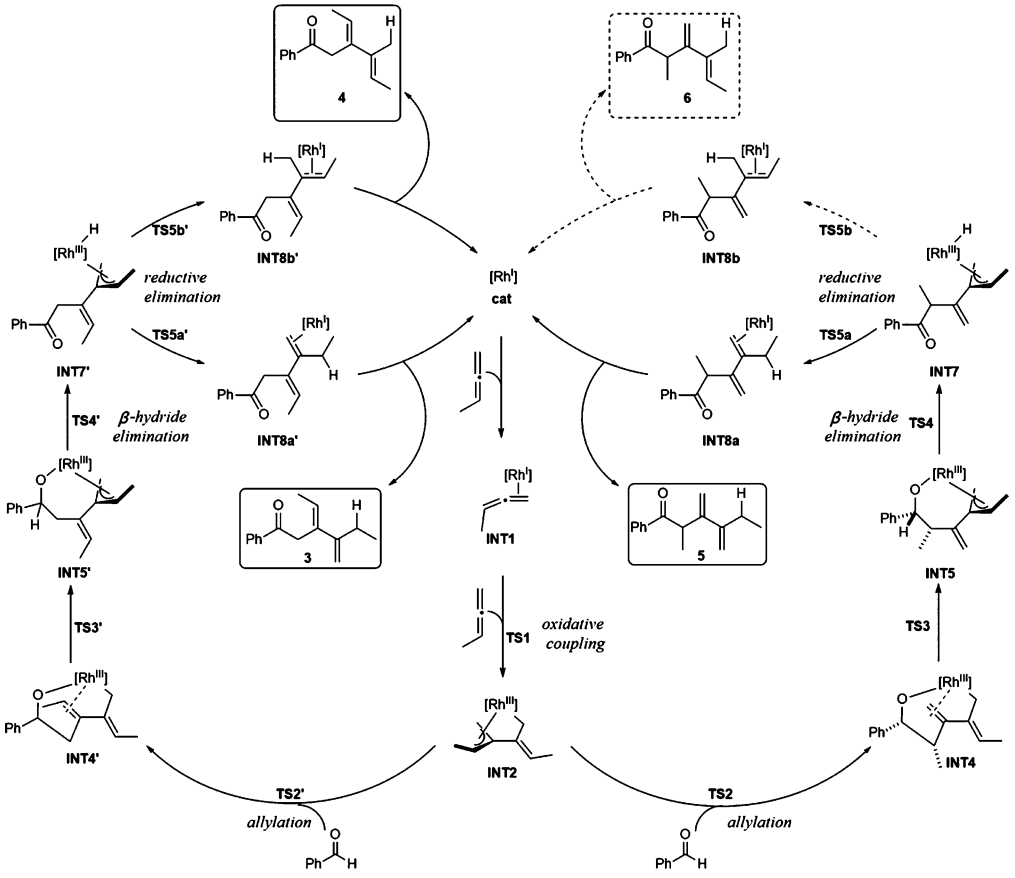

TS-RE′) was found to be 26.9 kcal/mol, which is 16.8 kcal/mol higher than for the β-elimination from the same intermediate (Figure 5). Hence, the C−O bond-forming reductive elimination should not take place, which is indeed the result observed experimentally.

3.4. Reductive Elimination. The last step of the mechanism, closing the catalytic cycle, is the C−H bond-forming reductive elimination (Scheme 3). This could occur directly from **INT6** and **INT6′**. The calculated free energy barriers are quite feasible (20.4 and 19.2 kcal/mol from **INT6**

dx.doi.org/10.1021/ja4014166 | J. Am. Chem. Soc. 2013, 135, 7647−7659

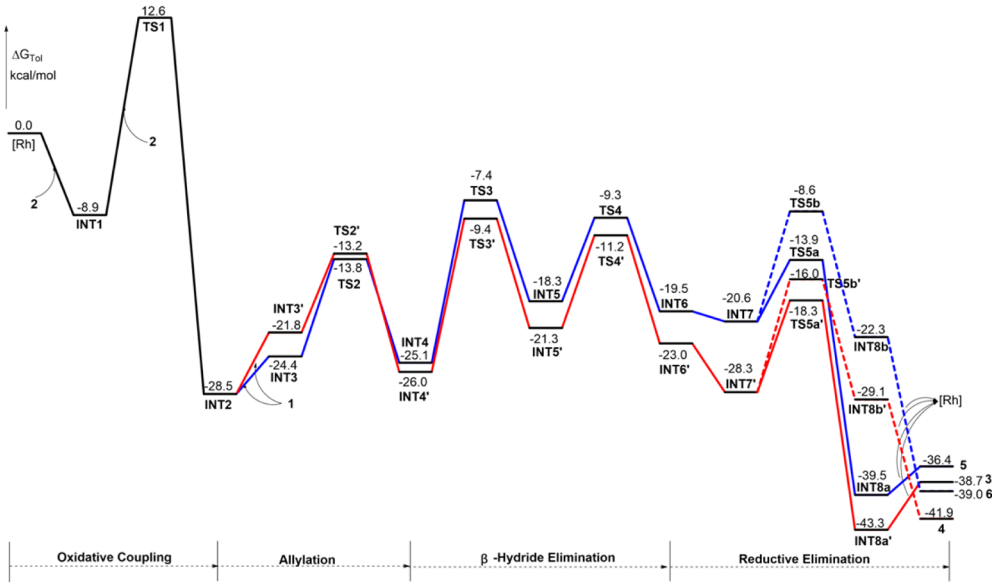

Figure 9. Free energy profile for the [RhCl(dppe)]-catalyzed 1:2 coupling of aldehydes and allenes.

and **INT6′**, respectively; see the Supporting Information for the optimized structures of the TSs). However, if the reaction were to follow this pathway, it would yield only compounds **4** and **5** as products rather than the experimentally observed mixture containing predominantly their isomer **3**. Prompted by this apparent flaw, we envisioned that the η^1-allylic complexes **INT6** and **INT6′** could be converted into their η^3-allylic counterparts **INT7** and **INT7′**, respectively, upon dissociation of the carbonyl oxygen from the rhodium center prior to the reductive elimination. The fact that both terminal carbon atoms of the η^3-allyl systems in **INT7** and **INT7′** can couple with the hydride during the reductive elimination would enable the formation of **3** in such a transformation.

Indeed, as shown in Figure 7, the Rh(III) hydrides containing the η^3-allyl ligand, **INT7** and **INT7′** (see Figure 8 for the structures), are more stable than **INT6** and **INT6′** by 1.1 and 5.3 kcal/mol, respectively.[24] As mentioned above, from **INT7** and **INT7′** the reductive elimination can occur at either the C1 or C3 side of the η^3-allyl. The calculations showed that irrespective of the starting complex, the reductive elimination engaging the methyl-substituted carbon C3 (**TS5a** and **TS5a′**) is more favorable than the one occurring at the unsubstituted carbon C1 (**TS5b** and **TS5b′**; Figure 7). This is typical behavior in many Rh-catalyzed reactions involving π-allyl species, which usually afford the branched product.[19a−m] One reason for this preference is that in **TS5a** and **TS5a′** the sterically crowded rhodium center is positioned closer to the less-substituted double bond (between C1 and C2). For example, in **TS5a′**, the bond distances of Rh−C1 and Rh−C2 are 2.15 and 2.16 Å, respectively, whereas in **TS5b′**, because of the steric effect of methyl group, the Rh−C2 and Rh−C3 bond distances are somewhat longer (2.19 and 2.22 Å, respectively) (Figure 8). Importantly, the free energies of all of the **TS5** variants are lower than those of the transition states for the direct reductive elimination from **INT6** and **INT6′**, implying that the reaction does not follow the latter pathway.[25] The influence of the relative energies of the reductive elimination transition states on the overall selectivity of the reaction will be discussed in the following section.

3.5. Overall Catalytic Cycle and Origins of the Regioselectivity in the [RhCl(dppe)]-Catalyzed Reaction.

The mechanism of the reaction as established by the present DFT calculations is summarized in Scheme 6, and the corresponding overall free energy profile is given in Figure 9. The catalytic cycle consists of four steps: (1) oxidative coupling of two allene molecules, (2) allylation of the aldehyde, (3) β-hydride elimination, and (4) C−H bond-forming reductive elimination. A prominent role in the mechanism is played by allylrhodium complexes. Because of the flexibility of the allyl ligand binding modes (η^3, η^1), a variety of reactivity patterns at each step of the catalytic cycle are available. Hence, the mechanism of the reaction involving allenes displays considerable differences compared with the mechanism of the related reductive coupling of acetylene and aldehyde shown in Scheme 2a,[9] in which vinyl ligands limited only to σ bonding are involved.

The oxidative coupling of two allene molecules (**TS1**) is a common step in all of the pathways leading to the experimentally observed products **3**−**5**. It has a barrier of 21.5 kcal/mol relative to the most stable Rh(I) complex, **INT1**. The oxidative coupling is irreversible and leads selectively to the octahedral η^3,η^1-bis(allylic) Rh(III) complex **INT2**, which has a well-defined and stable stereochemical configuration. Therefore, in this step of the mechanism, a number of structural features of the products are already determined, such as the C2−C2 linkage and the configuration of the double bonds. It is also important to point out that the overall barrier for the oxidative coupling is the highest among all of the barriers in the catalytic cycle. This step therefore constitutes the rate-determining step of the reaction.

Upon coordination of an aldehyde molecule, **INT2** undergoes a transformation to either **INT3** or **INT3′**, depending on which side of the η^3-allyl ligand remains bound to the metal (C1 or C3, respectively). Thus, this step constitutes the first divergence point, from which the two pathways proceed through the subsequent steps separately. The following step is the allylation of the aldehyde, which proceeds through the six-membered cyclic transition states **TS2** and **TS2′**. After an isomerization (**INT4** → **INT5** via **TS3** and **INT4′** → **INT5′**

dx.doi.org/10.1021/ja4014166 | J. Am. Chem. Soc. 2013, 135, 7647−7659

Scheme 7. Summary of the Mechanism of the [Rh(dppe)]$^+$-Catalyzed 1:2 Coupling of Aldehydes and Allenes

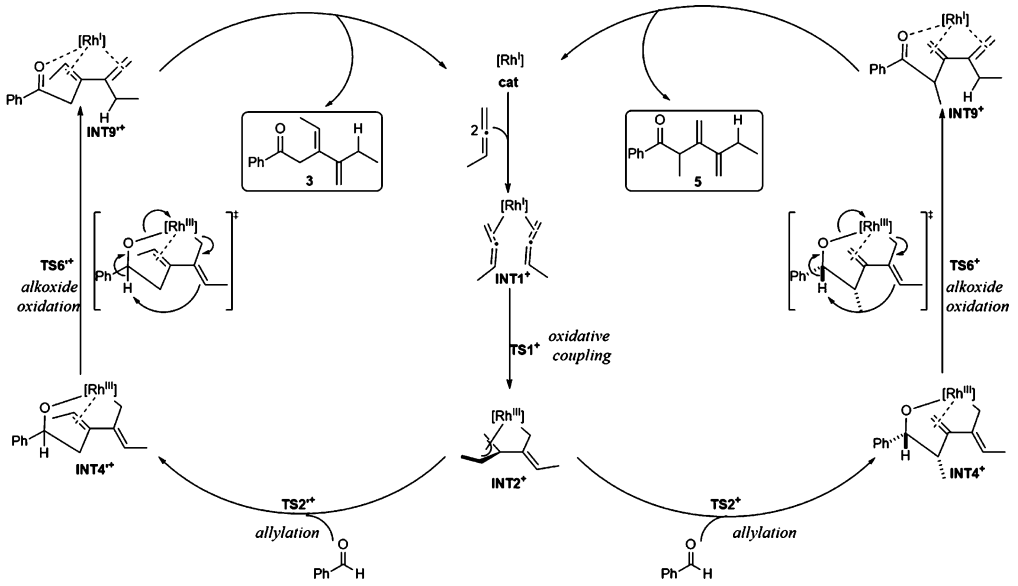

via **TS3′**) that is needed to create an empty coordination site in an appropriate position of the complex, a β-hydride elimination takes place via **TS4** and **TS4′**. Since **TS3** and **TS3′** are higher in energy than all of the subsequent transition states, passing them can be considered practically irreversible. Therefore, the ratio at which the catalyst is split to follow either one or the other branch of the catalytic cycle is determined by the free energy difference between the transition states **TS3** and **TS3′**. According to the calculations, these free energies differ by 2.0 kcal/mol, and hence, intermediates **INT6** and **INT6′** are formed in a 5:95 ratio.[26]

The next step of the mechanism is the C−H bond-forming reductive elimination, which starts with conversion of the η^1-allylic Rh(III) hydrides **INT6** and **INT6′** to the η^3-allylic species **INT7** and **INT7′**, respectively. The reductive elimination is the final regioselectivity-determining step. This process was found to take place preferentially at the C3 position (**TS5a** and **TS5a′**) rather than at C1 (**TS5b** and **TS5b′**). In particular, from **INT7′**, the formation of **INT8a′** via **TS5a′** is favored over the formation of **INT8b′** via **TS5b′** by 2.3 kcal/mol. This free energy difference corresponds approximately to a 98:2 ratio. On the other hand, the 5.3 kcal/mol free energy difference between **TS5a** and **TS5b** implies the practically exclusive transformation of **INT7** into **INT8a**. Hence, when the previous split of the reaction pathways is taken into account, the overall selectivity predicted by the calculations is **3**:**4**:**5** = 93:2:5, which is in very good agreement with the experimentally observed ratio of 91:6:3 (Scheme 2b).[6]

Finally, intermediates **INT8a′**, **INT8b′**, and **INT8a** formed in the reductive elimination regenerate the free catalyst [RhCl(dppe)] by releasing the corresponding products **3**, **4**, and **5**, respectively, closing the catalytic cycle. It should be pointed out that the relative stabilities of the free products **3**, **4**, and **5** do not correlate at all with their ratios resulting from the catalyzed reaction.

In summary, the above considerations show that the calculated energies can reproduce and rationalize the observed selectivity of the [RhCl(dppe)]-catalyzed reaction, which provides further support for the reaction mechanism suggested in Scheme 6.

3.6. Regioselectivity in the [Rh(dppe)]$^+$-Catalyzed Reaction. As mentioned in the Introduction, the selectivity of the reaction can be altered by replacing the chloride anion in the catalyst precursor with a noncoordinating counterion such as TfO$^-$, BF_4^-, or PF_6^-. To rationalize this catalyst-dependent selectivity, we reinvestigated the reaction mechanism with the cationic [Rh(dppe)]$^+$ complex as the active species. The calculations suggested that the cationic catalyst promotes a partially different mechanistic pathway (see Scheme 7 for the mechanism and Figure 10 for calculated energy profile), which in turn causes the alteration of the selectivity.

The first two steps of the mechanism are the same as for the [RhCl(dppe)] catalyst, except for the fact that because of the availability of an extra coordination site in the cationic catalyst, the initial **INT1**$^+$ complex contains two allene molecules. The

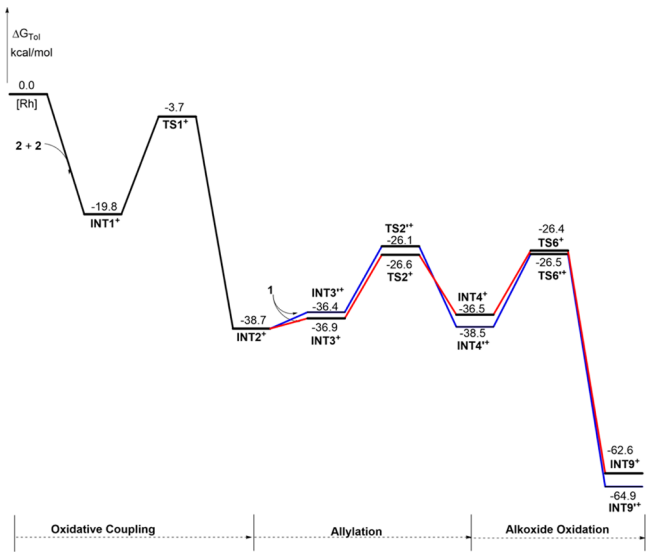

Figure 10. Free energy profile for the [Rh(dppe)]$^+$-catalyzed 1:2 coupling of aldehydes and allenes.

dx.doi.org/10.1021/ja4014166 | J. Am. Chem. Soc. 2013, 135, 7647−7659

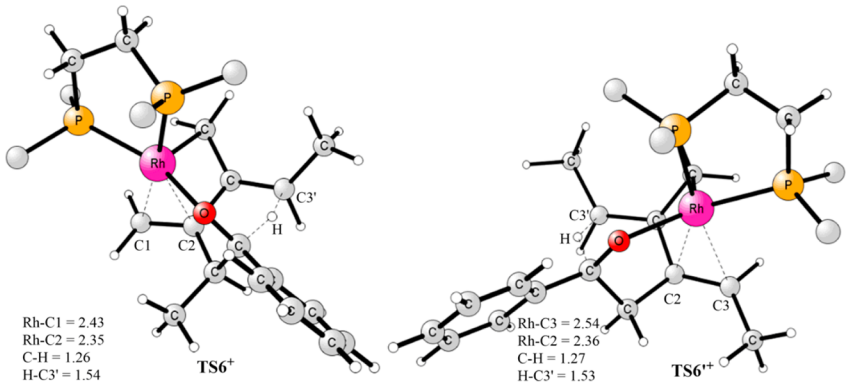

Figure 11. Optimized structures of the alkoxide oxidation transition states **TS6**$^+$ and **TS6′**$^+$.

reaction starts with oxidative coupling of the two allene moieties (**TS1**$^+$), resulting in the selective formation of η^3,η^1-bis(allylic) complex **INT2**$^+$. The structure of the allylic ligand in **INT2**$^+$ is identical to that in **INT2**, thus limiting the possible reaction products to **3**−**6** as discussed above for the neutral [RhCl(dppe)] catalyst. It should be noted that this step is also rate-determining for this catalyst. The next step is allylation of the aldehyde via **TS2**$^+$ and **TS2′**$^+$, resulting in intermediates **INT4**$^+$ and **INT4′**$^+$, respectively. The selectivity of the allylation is the same as before, that is, the allylation occurs preferentially at the C3 position via **TS2**$^+$.

From **INT4**$^+$ and **INT4′**$^+$, the reaction can follow the same isomerization/β-hydride elimination/reductive elimination pathway found for the neutral catalyst. The optimized geometries and calculated energy profile for this scenario are given in the Supporting Information. Similarly to the neutral catalyst, the highest barrier was calculated to occur for the isomerization (**TS3**$^+$ and **TS3′**$^+$), amounting to 12.0 and 12.2 kcal/mol relative to **INT4**$^+$ and **INT4′**$^+$, respectively. However, although the energy barriers are feasible, if such an analogous pathway were followed, it would lead to the same selectivity as before (i.e., predominantly product **3**; see the Supporting Information). This is in conflict with the experimental findings, which thus speaks against such a mechanism for the cationic catalyst.

Instead, we discovered an alternative mechanism that reproduces the reversed selectivity observed with the cationic catalyst. The alkoxide ligand present in the Rh(III) complexes **INT4**$^+$ and **INT4′**$^+$ can undergo a feasible direct oxidation to give the corresponding ketones (**TS6**$^+$ and **TS6′**$^+$; see Figure 11 for the optimized structures). In the course of the reaction, Rh(III) is reduced to Rh(I) and the final products **3** and **5** are formed directly (coordinated to the metal as **INT9′**$^+$ and **INT9**$^+$, respectively). A key role in this process is played by the η^1-allyl ligand, which acts as an internal base to abstract a proton from the alkoxide (Figure 11). Although perhaps somewhat surprising in this context, this transformation is analogous to the well-known oxidation of alcohols by high-valent metals, such as Mn(VII) and Cr(VI).[27] The example of related oxidation in Pd(II) complexes has also been reported.[28]

The barriers for **TS6**$^+$ and **TS6′**$^+$ relative to **INT4**$^+$ and **INT4′**$^+$, respectively, were calculated to be 10.1 and 12.0 kcal/mol, respectively. As shown in the free energy profile in Figure 10, the regioselectivity in this case is controlled by the free energy difference between **TS2′**$^+$ and **TS6**$^+$, which constitute the first irreversible steps in the respective pathways leading to the two products. The calculated free energy difference between these transition states is 0.3 kcal/mol, corresponding to a **3**:**5** ratio of 40:60.

Although the difference in the free energy barriers for the isomerization/β-hydride elimination/reductive elimination pathway (12.0 and 12.2 kcal/mol for **TS3**$^+$ and **TS3′**$^+$, respectively) and the alkoxide oxidation pathway (10.1 and 12.0 kcal/mol for **TS6**$^+$ and **TS6′**$^+$, respectively) is not so large that the former one can be completely ruled out, the fact that the alkoxide oxidation mechanism can account for the reversal of selectivity in the cationic catalyst is a strong argument in favor of it. Another piece of evidence is that the alkoxide oxidation via **TS6**$^+$ and **TS6′**$^+$ leads directly to compounds **3** and **5**, which explains why these are the only products observed experimentally in the reaction involving the cationic catalyst, while for the neutral catalyst, on the other hand, three products are observed.

Finally, it should be mentioned that we also located transition states for a similar alkoxide oxidation mechanism in the chloride-containing neutral complexes **INT4** and **INT4′**. However, the barriers were found to be much higher than those in the isomerization/β-hydride elimination/reductive elimination pathway discussed above (see the Supporting Information for details). Hence, the electron-deficient character of rhodium in the cationic complex is crucial for the alkoxide oxidation reaction.

4. CONCLUSIONS

The rhodium-catalyzed 1:2 coupling of aldehydes and allenes has been investigated in detail by DFT calculations. The free energy profiles for several possible reaction pathways have been calculated and compared.

For the reaction catalyzed by the neutral [RhCl(dppe)] complex, it has been shown that the energetically most plausible catalytic cycle consists of the following steps: oxidative coupling of the two allenes, allylation of the aldehyde, β-hydride elimination, and finally reductive elimination. The first step was found to be rate-determining for the overall reaction, and it leads to the formation of a bis(allylic) Rh(III) complex. Because of its ability to adopt either an η^3 or η^1 configuration, the allyl ligand turns out to play a key role throughout the mechanism, with profound consequences for the reaction selectivity.

The calculations showed that the remarkable regioselectivity of the reaction is an overall result of a number of selection events that take place in the catalytic cycle. The first regioselectivity-determining step is the oxidative coupling, in which the C2−C2 linkage between the allene moieties is

dx.doi.org/10.1021/ja4014166 | J. Am. Chem. Soc. 2013, 135, 7647−7659

selectively established. Subsequently, the selectivity of the second C−C bond formation is controlled during the β-hydride elimination. Finally, the reductive elimination was found to yield the branched product preferentially.

For the reaction catalyzed by the cationic $[Rh(dppe)]^+$ complex, on the other hand, the calculations suggested a different reaction mechanism after the allylation step. Namely, oxidation of the alkoxide can take place directly to yield the products. This important difference explains the experimentally observed reversal of selectivity.

The present calculations thus provide important insights into the mechanism of rhodium(I)-catalyzed coupling reactions, in particular those involving allenes, and will have a general bearing on the improvement of existing catalytic systems and the design of new ones.

■ ASSOCIATED CONTENT

Supporting Information

Complete ref 13, additional results not shown in the text, and Cartesian coordinates of all optimized structures discussed in the paper. This material is available free of charge via the Internet at http://pubs.acs.org.

■ AUTHOR INFORMATION

Corresponding Author

himo@organ.su.se

Notes

The authors declare no competing financial interest.

■ ACKNOWLEDGMENTS

We acknowledge financial support from the Swedish Research Council, the Göran Gustafsson Foundation, and the Knut and Alice Wallenberg Foundation. G.H. thanks the Carl Trygger Foundation for a postdoctoral fellowship. Computer time was generously provided by the Swedish National Infrastructure for Computing.

■ REFERENCES

(1) (a) Lautens, M.; Klute, W.; Tam, W. *Chem. Rev.* **1996**, *96*, 49−92. (b) Kotha, S.; Brahmachary, E.; Lahiri, K. *Eur. J. Org. Chem.* **2005**, 4741−4767. (c) Murakami, M. *Angew. Chem., Int. Ed.* **2003**, *42*, 718−720. (d) Inglesby, P. A.; Evans, P. A. *Chem. Soc. Rev.* **2010**, *39*, 2791−2805. (e) Shibata, T.; Tsuchikama, K. *Org. Biomol. Chem.* **2008**, *6*, 1317−1323. (f) Tanaka, K. *Chem.—Asian J.* **2009**, *4*, 508−518. (g) Yu, Z.-X.; Wang, Y.; Wang, Y. *Chem.—Asian J.* **2010**, *5*, 1072−1088.

(2) (a) Willis, M. C. *Chem. Rev.* **2010**, *110*, 725−748. (b) Jun, C.-H.; Moon, C. W.; Lee, D.-Y. *Chem.—Eur. J.* **2002**, *8*, 2422−2428. (c) Leung, J. C.; Krische, M. J. *Chem. Sci.* **2012**, *3*, 2202−2209.

(3) (a) Jang, H.-Y.; Krische, M. J. *Acc. Chem. Res.* **2004**, *37*, 653−661. (b) Ngai, M.-Y.; Kong, J.-R.; Krische, M. J. *J. Org. Chem.* **2007**, *72*, 1063−1072. (c) Iida, H.; Krische, M. J. *Top. Curr. Chem.* **2007**, *279*, 77−104. (d) Bower, J. F.; Kim, I. S.; Patman, R. L.; Krische, M. J. *Angew. Chem., Int. Ed.* **2009**, *48*, 34−46. (e) Skucas, E.; Ngai, M.-Y.; Komanduri, V.; Krische, M. J. *Acc. Chem. Res.* **2007**, *40*, 1394−1401.

(4) Kong, J. R.; Krische, M. J. *J. Am. Chem. Soc.* **2006**, *128*, 16040−16041.

(5) The reaction scope was later expanded by inclusion of other aldehydes and imines as coupling partners. See: (a) Skucas, E.; Kong, J. R.; Krische, M. J. *J. Am. Chem. Soc.* **2007**, *129*, 7242−7243. (b) Han, S. B.; Kong, J. R.; Krische, M. J. *Org. Lett.* **2008**, *10*, 4133−4135.

(6) Toyoshima, T.; Miura, T.; Murakami, M. *Angew. Chem., Int. Ed.* **2011**, *50*, 10436−10439.

(7) (a) Oonishi, Y.; Hosotani, A.; Sato, Y. *J. Am. Chem. Soc.* **2011**, *133*, 10386−10389. (b) Hojo, D.; Tanaka, K. *Org. Lett.* **2012**, *14*, 1492−1495.

(8) The total of 36 refers only to the number of possible linear compounds containing the reactant molecules coupled in a aldehyde−allene−allene sequence. In fact, two of the above isomers contain two asymmetric carbon atoms and hence can exist as two diastereomers, raising the number of possible products with distinct energies to 38. If cyclic structures and those containing allene−aldehyde−allene sequence are also considered, the number of possible products is even greater.

(9) Williams, V. M.; Kong, J. R.; Ko, B. J.; Mantri, Y.; Brodbelt, J. S.; Baik, M.-H.; Krische, M. J. *J. Am. Chem. Soc.* **2009**, *131*, 16054−16062.

(10) Miura, T.; Biyajima, T.; Toyoshima, T.; Murakami, M. *Beilstein J. Org. Chem.* **2011**, *7*, 578−581.

(11) In fact, to the best of our knowledge, all of the transition-metal-catalyzed $[n + m + o]$ cycloadditions involving allenes developed to date incorporate only one or two molecules of allene into the product. See: (a) Murakami, M.; Ubukata, M.; Itami, K.; Ito, Y. *Angew. Chem., Int. Ed.* **1998**, *37*, 2248−2250. (b) Shanmugasundaram, M.; Wu, M.-S.; Cheng, C.-H. *Org. Lett.* **2001**, *3*, 4233−4236. (c) Shanmugasundaram, M.; Wu, M.-S.; Jeganmohan, M.; Huang, C.-W.; Cheng, C.-H. *J. Org. Chem.* **2002**, *67*, 7724−7729. (d) Miura, T.; Morimoto, M.; Murakami, M. *J. Am. Chem. Soc.* **2010**, *132*, 15836−15838. (e) Brusoe, A. T.; Alexanian, E. J. *Angew. Chem., Int. Ed.* **2011**, *50*, 6596−6600.

(12) (a) McCarren, P. R.; Liu, P.; Cheong, P. H.-Y.; Jamison, T. F.; Houk, K. N. *J. Am. Chem. Soc.* **2009**, *131*, 6654−6655. (b) Liu, P.; McCarren, P.; Cheong, P. H.-Y.; Jamison, T. F.; Houk, K. N. *J. Am. Chem. Soc.* **2010**, *132*, 2050−2057. (c) Liu, P.; Krische, M. J.; Houk, K. N. *Chem.—Eur. J.* **2011**, *17*, 4021−4029.

(13) Frisch, M. J.; et al. *Gaussian 03*, revision D.01; Gaussian, Inc.: Wallingford, CT, 2004.

(14) (a) Becke, A. D. *J. Chem. Phys.* **1993**, *98*, 5648−5652. (b) Lee, C. T.; Yang, W. T.; Parr, R. G. *Phys. Rev. B* **1988**, *37*, 785−789.

(15) Hay, P. J.; Wadt, W. R. *J. Chem. Phys.* **1985**, *82*, 270−283.

(16) (a) Barone, V.; Cossi, M. *J. Phys. Chem. A* **1998**, *102*, 1995−2001. (b) Cossi, M.; Rega, N.; Scalmani, G.; Barone, V. *J. Comput. Chem.* **2003**, *24*, 669−681.

(17) Grimme, S. *J. Comput. Chem.* **2006**, *27*, 1787−1799.

(18) For instance, see: (a) Minenkov, Y.; Occhipinti, G.; Jensen, V. R. *J. Phys. Chem. A* **2009**, *113*, 11833−11844. (b) Siegbahn, P. E. M.; Blomberg, M. R. A.; Chen, S.-L. *J. Chem. Theory Comput.* **2010**, *6*, 2040−2044. (c) Harvey, J. N. *Faraday Discuss.* **2010**, *145*, 487−505. (d) McMullin, C. L.; Jover, J.; Harvey, J. N.; Fey, N. *Dalton Trans.* **2010**, *39*, 10833−10836. (e) Lonsdale, R.; Harvey, J. N.; Mulholland, A. J. *J. Phys. Chem. Lett.* **2010**, *1*, 3232−3237. (f) Osuna, S.; Swart, M.; Solà, M. *J. Phys. Chem. A* **2011**, *115*, 3491−3496. (g) Santoro, S.; Liao, R.-Z.; Himo, F. *J. Org. Chem.* **2011**, *76*, 9246−9252. (h) Nordin, M.; Liao, R.-Z.; Ahlford, K.; Adolfsson, H.; Himo, F. *ChemCatChem* **2012**, *4*, 1095−1104. (i) Xu, X.; Liu, P.; Lesser, A.; Sirois, L. E.; Wender, P. A.; Houk, K. N. *J. Am. Chem. Soc.* **2012**, *134*, 11012−11025. (j) Jiménez-Halla, J. O. C.; Kalek, M.; Stawinski, J.; Himo, F. *Chem.—Eur. J.* **2012**, *18*, 12424−12436. (k) Kalek, M.; Himo, F. *J. Am. Chem. Soc.* **2012**, *134*, 19159−19169. (l) Huang, G.; Xia, Y.; Sun, C.; Li, J.; Lee, D. *J. Org. Chem.* **2013**, *78*, 988−995.

(19) For selected reports of η^3-allyl Rh species, see: (a) Evans, P. A.; Lawler, M. J. *J. Am. Chem. Soc.* **2004**, *126*, 8642−8643. (b) Evans, P. A.; Leahy, D. K. *Chemtracts* **2003**, *16*, 567−578. (c) Evans, P. A.; Leahy, D. K.; Slieker, L. M. *Tetrahedron: Asymmetry* **2003**, *14*, 3613−3618. (d) Evans, P. A.; Robinson, J. E.; Moffett, K. K. *Org. Lett.* **2001**, *3*, 3269−3271. (e) Arnold, J. S.; Cizio, G. T.; Nguyen, H. M. *Org. Lett.* **2011**, *13*, 5576−5579. (f) Arnold, J. S.; Cizio, G. T.; Heitz, D. R.; Nguyen, H. M. *Chem. Commun.* **2012**, *48*, 11531−11533. (g) Arnold, J. S.; Stone, R. F.; Nguyen, H. M. *Org. Lett.* **2010**, *12*, 4580−4583. (h) Arnold, J. S.; Nguyen, H. M. *J. Am. Chem. Soc.* **2012**, *134*, 8380−8383. (i) Hayashi, T.; Okada, A.; Suzuka, T.; Kawatsura, M. *Org. Lett.* **2003**, *5*, 1713−1715. (j) Vrieze, D. C.; Hoge, G. S.; Hoerter, P. Z.; Van Haitsma, J. T.; Samas, B. M. *Org. Lett.* **2009**, *11*, 3140−3142. (k) Koschker, P.; Lumbroso, A.; Breit, B. *J. Am. Chem. Soc.* **2011**, *133*, 20746−20749. (l) Lumbroso, A.; Koschker, P.; Vautravers, N. R.; Breit, B. *J. Am. Chem. Soc.* **2011**, *133*, 2386−2389. (m) Nishimura, T.; Hirabayashi, S.; Yasuhara, Y.; Hayashi, T. *J. Am. Chem. Soc.* **2006**, *128*,

2556−2557. (n) Choi, J.-c.; Osakada, K.; Yamamoto, T. *Organometallics* **1998**, *17*, 3044−3050. (o) Barros, H. J. V.; Guimarães, C. C.; dos Santos, E. N.; Gusevskaya, E. V. *Organometallics* **2007**, *26*, 2211−2218. (p) Jiao, L.; Lin, M.; Zhuo, L.-G.; Yu, Z.-X. *Org. Lett.* **2010**, *12*, 2528−2531. (q) Jiao, L.; Lin, M.; Yu, Z.-X. *J. Am. Chem. Soc.* **2011**, *133*, 447−461. (r) Lin, M.; Li, F.; Jiao, L.; Yu, Z.-X. *J. Am. Chem. Soc.* **2011**, *133*, 1690−1693. (s) Lin, M.; Kang, G.-Y.; Guo, Y.-A.; Yu, Z.-X. *J. Am. Chem. Soc.* **2012**, *134*, 398−405. (t) Li, Q.; Yu, Z.-X. *Organometallics* **2012**, *31*, 5185−5195.

(20) (a) Szabó, K. J. *Chem.—Eur. J.* **2004**, *10*, 5268−5275. (b) Szabó, K. J. *Chem.—Eur. J.* **2000**, *6*, 4413−4421.

(21) There is an additional possibility of a migratory insertion of a third molecule of allene instead of the aldehyde. Such a pathway would eventually lead to [2 + 2 + 2] trimerization of the allene. However, since experimentally allene **2** only dimerizes (see ref 10), this possibility was not considered computationally.

(22) For selected reviews of allylation of carbonyl compounds, see: (a) Denmark, S. E.; Fu, J. *Chem. Rev.* **2003**, *103*, 2763−2794. (b) Kennedy, J. W. J.; Hall, D. G. *Angew. Chem., Int. Ed.* **2003**, *42*, 4732−4739. (c) Yu, C.-M.; Youn, J.; Jung, H.-K. *Bull. Korean Chem. Soc.* **2006**, *27*, 463−472. (d) Marek, I.; Sklute, G. *Chem. Commun.* **2007**, 1683−1691. (e) Hall, D. G. *Synlett* **2007**, 1644−1655.

(23) For examples of [2 + 2 + 2] cyclization involving carbonyl compounds, see: (a) Tsuchikama, K.; Yoshinami, Y.; Shibata, T. *Synlett* **2007**, 1395−1398. (b) Tanaka, K.; Otake, Y.; Wada, A.; Noguchi, K.; Hirano, M. *Org. Lett.* **2007**, *9*, 2203−2206.

(24) Transition states connecting **INT6** to **INT7** and **INT6′** to **INT7′** could not be optimized. However, energy scans showed that the barriers are quite low, much lower than those for the direct reductive elimination (see the Supporting Information).

(25) The methyl group in the η^3-allyl complexes **INT7** and **INT7′**, contrary to the case of **INT2** discussed above, can undergo a relocation from the anti position to the syn position. This could potentially lead to the formation of isomers of products **4** and **6** containing different configurations at one of the double bonds. However, the barriers for the syn/anti substituent exchange in **INT7** and **INT7′** were calculated to be much higher than those for the reductive elimination. Therefore, **INT7** and **INT7′** undergo the reductive elimination before they can isomerize. See the Supporting Information for details.

(26) The ratios were calculated using the Eyring equation. For example, the ratio of **INT6** to **INT6′** was calculated as

$$\frac{\mathbf{INT6}}{\mathbf{INT6'}} = e^{[\Delta G_{Tol}(\mathbf{TS3}) - \Delta G_{Tol}(\mathbf{TS3'})]/RT}$$

(27) Wade, L. G. Jr. *Organic Chemistry*, 6th ed.; Prentice-Hall: Upper Saddle River, NJ, 2006.

(28) Nielsen, R. J.; Goddard, W. A., III. *J. Am. Chem. Soc.* **2006**, *128*, 9651−9660.